

Depth-dependent critical behavior in V₂H

Charo I. Del Genio,^{1,2} Johann Trenkler,^{1,3,*} Kevin E. Bassler,^{1,2} Peter Wochner,³
Dean R. Haeffner,⁴ George F. Reiter,¹ Jianming Bai,⁵ and Simon C. Moss^{1,2}

¹*University of Houston, Department of Physics, 617 Science & Research 1, 4800 Calhoun Rd, Houston, TX 77204-5005*

²*Texas Center for Superconductivity, Houston, TX 77204*

³*Max Planck Institut für Metallforschung, D-70569 Stuttgart, Germany*

⁴*Advanced Photon Source, Argonne National Laboratory, Argonne, IL 60439-4815*

⁵*Oak Ridge National Laboratory, Oak Ridge, TN 37831*

(Dated: June 8, 2018)

Using X-ray diffuse scattering, we investigate the critical behavior of an order-disorder phase transition in a defective “skin-layer” of V₂H. In the skin-layer, there exist walls of dislocation lines oriented normal to the surface. The density of dislocation lines within a wall decreases continuously with depth. We find that, because of this inhomogeneous distribution of defects, the transition effectively occurs at a depth-dependent local critical temperature. A depth-dependent scaling law is proposed to describe the corresponding critical ordering behavior.

PACS numbers: 61.05.cp, 64.60.Cn, 64.60.F-, 64.60.Kw, 61.72.Dd

I. INTRODUCTION

Structural defects exist in almost all real crystalline solids. Therefore, in order to understand structural phase transitions, it is crucial to understand the influence that defects can have on ordering behavior. It has been shown that defects, through their accompanying strain fields, can change the nature of phase transitions, including their universal critical properties^{1,2}. Defects have also been shown to be responsible for the appearance of the so-called “central peak” in diffuse X-ray or neutron scattering and the related “two-length scale” phenomena observed in an number of experimental systems^{2,3,4,5,6,7,8,9,10,11,12,13}. These previous studies have implicitly assumed that defects are homogeneously distributed in the material, at least in the region of the crystal being studied, even if that region is only a “skin-layer”, i.e., a near-surface region in which the defect density is known to be different than in the bulk. In real systems, however, defects are often caused by surface treatments. In this case, they can be inhomogeneously distributed, occurring mostly in a skin-layer with a density that continuously decays into the bulk over several microns^{13,14,15}. Such an inhomogeneous distribution of defects complicates the ordering behavior of many real crystals. In this letter, using diffuse X-ray scattering in both reflection and transmission geometries, we analyze the depth-dependent critical behavior of the structural ordering of a crystal with this type of inhomogeneous defect distribution.

Divanadium hydride (V₂H) is an interstitial alloy that undergoes a structural phase transition between an ordered monoclinic phase β_1 and a disordered body centered tetragonal phase β_2 as temperature is increased (for the phase diagram see Ref. 16). In the crystal we study, defects occur almost exclusively in a skin-layer that extends several μm below the surface. In the skin-layer, there exist walls of dislocation lines oriented normal to the surface¹⁵. The density of dislocation lines in the walls

decreases with depth. As we will see, the character of the structural transition in the crystal can change radically with the depth at which it takes place. In the bulk material it is first order¹⁷, but it becomes continuous in the skin-layer and has a critical temperature and critical properties that depend on depth. We propose a modification of the scaling law for the inverse correlation length that accounts for its depth-dependence and allows us to treat the scattering measurements at different depths in a unified framework.

II. EXPERIMENTAL SETUP AND RESULTS

For our experiments we used a thin plate (0.96 mm) of a vanadium single crystal loaded with purified hydrogen, so that it had a bulk concentration ratio of $c_{\text{H}}/c_{\text{V}} = 0.525 \pm 0.005$. For sample preparation and analysis see Refs. 14 and 18. We performed X-ray experiments on the crystal in both reflection and transmission geometry. The reflection experiments were performed with MoK _{α 1} X-rays at a rotating anode source and at several energies on X14A at the NSLS at Brookhaven National Laboratory. The high energy transmission experiments were carried out with 44.1 keV X-rays at the undulator beamline SRI-CAT, 1-ID, at the APS at Argonne National Laboratory¹⁷. In all the experiments we confirmed the absence of higher harmonic contamination. Since we earlier observed two length scales in this crystal¹⁴ we used the different scattering geometries and energy ranges in order to detect separately the influences arising from the bulk and the skin layer. In all cases the sample was mounted in a strain-free manner in a vacuum of $\sim 10^{-4}$ torr. The temperature fluctuations of the entire setup were less than 0.05 K at $T > 443$ K.

We have four indications of a defective near-surface layer on our sample: (1) A hydrogen and oxygen gradient measured by high resolution elastic recoil detection analysis (HERDA) in the first 150 \AA ¹⁸; (2) an oxygen gra-

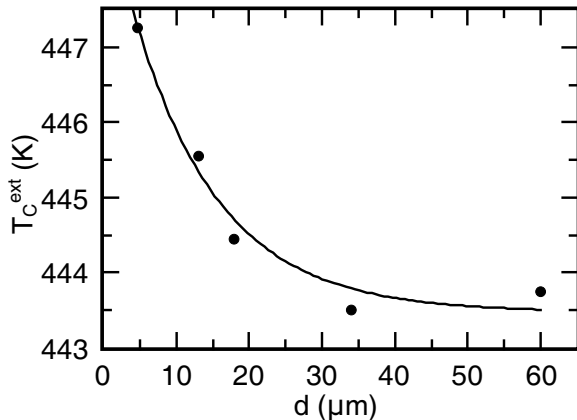


FIG. 1: Critical temperature T_C^{ext} versus depth d .

dient measured by secondary neutral mass spectroscopy (SNMS) in the first 150–200 Å¹⁸; (3) the decay of the mosaic spread with depth^{14,15}; (4) a larger d -spacing in the near-surface region than in the bulk¹⁴. HERDA shows that the hydrogen content increases with depth until the bulk concentration is reached at a depth of about 150 Å. In our most surface sensitive experiment we have used 9 keV X-rays and low momentum transfers to measure the influence of the upper 150 Å on the scattering; this contribution appears to be about 0.2 %, as deduced from the fraction R of the intensity diffracted down to a depth d in the sample. In a symmetric scattering geometry, R is given by

$$R = 1 - e^{-2\frac{\mu d}{\sin\Theta}}, \quad (1)$$

where μ is the linear absorption coefficient of X-rays and Θ is the Bragg angle¹⁹. The only defects penetrating up to several microns in our sample are thus the walls of dislocations responsible for the mosaic spread. We note that there is a depth-dependent stress field associated with this decay, caused by walls of dislocation lines¹⁵.

We focus here on the depth dependence of the critical behavior in the vicinity of the β_1 - β_2 order-disorder transition in the several micron thick skin-layer. The correlation length $\xi = 1/\kappa$ for $T \geq T_C^{ext}$ at a constant depth is the inverse of the half width at half maximum of the critical diffuse scattering (CDS) profiles, and could be reliably determined only through a fit involving a convolution of the measured resolution function and the CDS profiles. The critical temperature $T_C^{ext}(d)$, whose value depends on the depth d (see Fig. 1), is defined here as the extrapolated temperature at which the full width at half maximum reaches 0. Note that $T_C^{ext}(d)$ is an “integrated” quantity that depends on the scattering from the entire skin-layer down to depth d . The fact that $T_C^{ext}(d)$ depends on depth, presumably implies that there is a real, local critical temperature $\hat{T}_C(d)$ that also depends on depth. Note also that the concept of a local

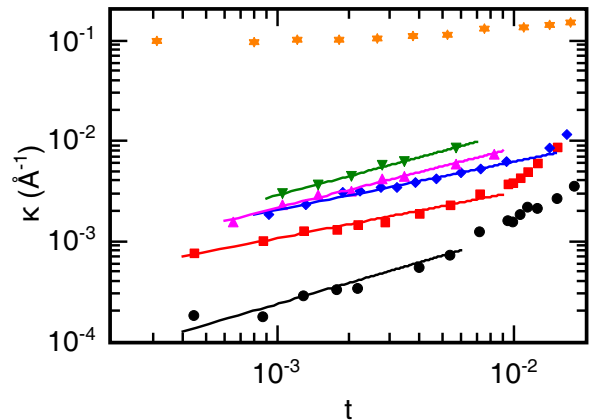


FIG. 2: (Color online) Inverse correlation length κ versus reduced temperature $t = \frac{T}{T_C^{ext}} - 1$ for different depths. The black circles correspond to 1.6 μm , the red squares to 13.1 μm , the blue diamonds to 18.4 μm , the pink upward triangles to 25 μm , the green downward triangles to 34 μm and the orange stars to the bulk.

critical temperature is well-defined only within a region smaller than the local correlation length. In other words, for any particular depth d^* , when the temperature approaches $T_C(d^*)$ the ordering process will happen in a layer around that depth not thicker than the local correlation length.

The high energy transmission experiments indicated a strong first order phase transition in the bulk, evidenced by a strong drop of the $(0 \ 5/2 \ \bar{5}/2)$ superstructure intensity by a factor of more than 400 at T_C^{ext} (see Ref. 17). This is associated with a transition width of ≈ 0.3 K, together with an abrupt broadening of the intensity profile at the superstructure position.

However, in the skin layer the transition is continuous and the long-range order parameter exponent β can be determined from the integrated Bragg intensities of superstructure reflections I :

$$I \propto \Phi^2 = -B \left(\frac{T}{T_C^{ext}} - 1 \right)^{2\beta}, \quad (2)$$

where Φ is the Bragg-Williams order parameter, and B a constant. From the corrected intensities for the $(0 \ 5/2 \ \bar{5}/2)$ and $(0 \ 7/2 \ \bar{7}/2)$ superstructure reflections, after excluding a small two-phase region, we obtained a value of $\beta = 0.18 \pm 0.02$ (see Ref. 18), treating T_C^{ext} as a fit parameter as, e.g., in Ref. 20.

Since κ scales generally as $\kappa = \kappa_0 t^\nu$, where here $t = \frac{T}{T_C^{ext}} - 1$ is the reduced temperature²¹, we estimated the correlation length exponent ν from the slope of a double logarithmic plot of the fitted κ versus t (Fig. 2); the values obtained were $0.48 \pm 0.05 \leq \nu \leq 0.58 \pm 0.07$ when neglecting the crossover in ν and in the susceptibility exponent γ at larger reduced temperatures¹⁴. The range in

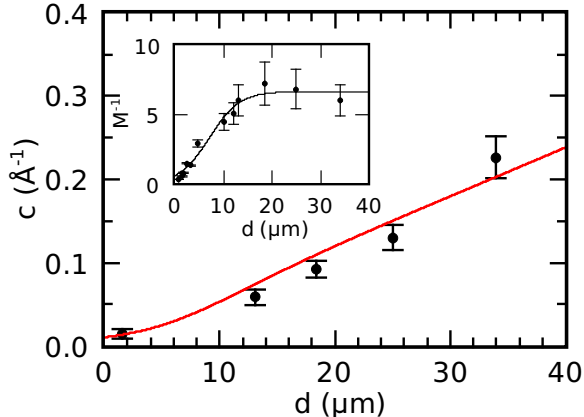


FIG. 3: (Color online) Proportionality factor c (eq. 3) vs. depth d . The solid red line is the value of c calculated according to eq. 8. Inset: inverse of the mosaic spread (dimensionless) versus depth d .

ν is essentially attributable to experimental uncertainties, e.g., the limited resolution for smaller t . Note that we measure essentially the same value of ν and of the other critical exponents regardless of depth. Thus, the value of the critical exponents are *depth-independent*.

Our values of β , ν and γ_1 (0.96 ± 0.13 as reported in Ref. 14) all support tricritical behavior in the skin layer for small t when the tricritical point is approached along the T -axis. Although the correlation length decreases with depth, our values of ν and γ_1 (the subscript “1” refers to small t) compare quite well with the theoretical values of $\nu = 0.5$ and $\gamma_1 = 1$ obtained from the analysis of a metamagnet which yields mean field exponents^{21,22}. They also compare well with other systems presumed to be tricritical, e.g., $\nu = 0.52 \pm 0.08$ and $\gamma_1 = 1.05 \pm 0.20$ for $\text{Nd}_4\text{Cl}^{23}$.

III. ANALYSIS AND THEORETICAL MODEL

According to the criteria defined by Krivoglaz²⁴, the composition of the sample was close enough to the tricritical point to observe tricritical behavior. Although the experimental value of β is smaller than the theoretically expected value of 0.25, it is comparable with an earlier measurement and with other tricritical systems if the influence of the two-phase region is neglected^{18,20}. Given this good agreement between the values for the critical exponent, we believe that tricritical behavior is dominant for small reduced temperatures.

Despite the fact that the critical exponent ν is depth-independent, there is a depth dependence to the measured behavior of the correlation length, or, equivalently, to the inverse correlation length κ . To account for this depth-dependence, we propose that the scaling law for κ

be modified such that

$$\kappa(d) = c(d) t^\nu, \quad (3)$$

where the factor c is dependent on the depth d . To determine the function $c(d)$ we calculated the y -intercepts of the fitted κ vs. t plots shown in Fig. 2. The resulting measured values for $c(d)$ are shown in Fig. 3.

These results indicate that, for the same change in t^ν , the inverse correlation length decreases faster for smaller depths. On the other hand, the critical ordering being measured is presumably occurring near the defect lines due to their strain fields^{1,2}, which cause the appearance of ordered regions. We can then safely assume that the density of ordered regions at any given depth is proportional to the density of dislocation lines at the same depth. The mosaic spread gives us a measure of this density, so we expect $c(d)$ to be proportional to the inverse of the mosaic spread. However, it should be noted that since $\kappa(d)$ is calculated from the half width of the CDS profiles at depth d , it is an averaged measure. In fact, the CDS profiles measure ordering throughout the skin-layer to the depth that is probed. Thus, arguably, $c(d)$ should be proportional to an integral average of the inverse of the mosaic spread M from the surface to depth d :

$$c(d) \propto \frac{1}{Z} \int_0^d \frac{1}{M(z)} dz. \quad (4)$$

The factor Z has to account for the absorption of the X-rays along the path through the material, so that it is, in itself, an integrated quantity:

$$Z(d) = \int_0^{l(d)} e^{-\mu x} dx, \quad (5)$$

where μ is the X-ray absorption coefficient and l is the effective path into the material, which, for a depth d and a scattering angle ϑ is given by

$$l(d) = \frac{2d}{\sin \vartheta}. \quad (6)$$

We can then express Z directly as

$$Z(d) = \frac{1}{\mu} \left(1 - e^{-2\mu d / \sin \vartheta} \right) \quad (7)$$

and, absorbing μ into the proportionality, give our final expression for the experimentally measured c as

$$c(d) \propto \frac{\int_0^d \frac{1}{M(z)} dz}{1 - e^{-2\mu d / \sin \vartheta}}. \quad (8)$$

This quantity, calculated with average values of μ and $\sin \vartheta$ and using a sigmoid function fit for M , is shown as a line in the main part of Fig. 3. The proportionality constant used, dependent on the particular sample and the details of the experiment, had a fitted value of 0.1 m^{-2} . In the inset of the same figure we show the depth dependence of the inverse of the mosaic spread. Notice also

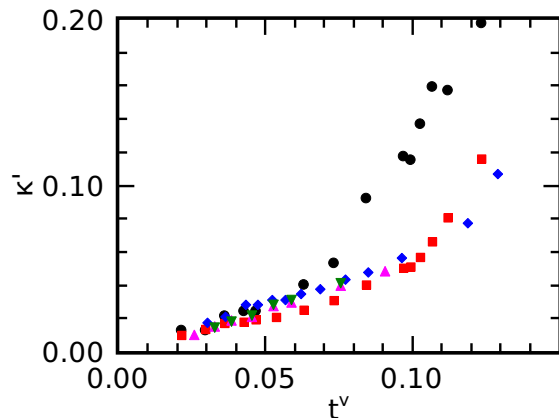


FIG. 4: (Color online) Inverse correlation scaling function κ' versus scaled reduced temperature t^ν , showing the data collapse. The black circles correspond to $1.6 \mu\text{m}$, the red squares correspond to $13.1 \mu\text{m}$, the blue diamonds to $18.4 \mu\text{m}$, the pink upward triangles to $25 \mu\text{m}$ and the green downward triangles to $34 \mu\text{m}$.

that in this estimate for the experimentally measured c , μ and $\sin \vartheta$ only play a significant role for small depths, due to their presence in a negative exponential.

With this treatment for $c(d)$, it is possible to collapse the scattering data for κ onto a single scaling function

$$\kappa' = \frac{\kappa}{c(d)} \quad (9)$$

as shown in Fig. 4. Note that when t^ν goes to 0 the collapsed curves extrapolate to 0. This corresponds to a vanishing inverse correlation length, or, equivalently, to a diverging correlation length and thus suggests that $T_C^{ext}(d)$ is the actual critical temperature, or at least that it is not too far from the real critical temperature $\hat{T}_C(d)$. The tails of the curves, for $t^\nu \gtrsim 0.07$ correspond to the critical region above the two-length scale crossover¹⁴.

The collapse is strong evidence that the density of defects directly drives the critical behavior in the material. The mechanism involved is very likely to be the interaction with the stress and strain fields induced by the defects, which is most probably also responsible for the crossover to different values of the critical exponents and for the change in the order of the transition between bulk and skin-layer.

IV. CONCLUSIONS

In summary, we have observed a change in the order of the phase transition in a V_2H crystal, which is first-order in the pure bulk and continuous in a skin layer that is several microns thick. Defects, in the form of dislocation lines, exist in the skin layer and are responsible for the change in the ordering behavior. The density of those defects is inhomogeneously distributed and decays continuously with depth from the surface. Throughout the skin layer, near the critical temperature, the measured values of the critical exponents are those of a tricritical point. Although the values of the critical exponents describing the scaling behavior of thermodynamic functions in the skin layer do not depend on depth, the coefficients of the power law function of κ and, presumably, of other thermodynamic functions, do show a depth dependence. Focusing on the behavior of κ , we find that its depth-dependent scaling coefficient depends on an integral average of the inverse defect density. Using this fact and postulating a modified scaling law for the inverse correlation length, we are able to collapse the measured data onto a single scaling function. Thus, we are able to treat scattering measurements at different depths in a single unified framework.

Acknowledgments

The authors would like to thank R. Hempelmann for loading the crystal used in these experiments and D. Lott, H. D. Carstanjen, P. C. Chow, D. De Fontaine, J. W. Cahn and R. Barabash for help in the experiment or fruitful discussions. Furthermore, we thank G. Srajer and the beamline personnel at the SRI-CAT at the APS at the Argonne National Laboratory for assistance during the experiment. The work of CIDG and KEB was supported by the NSF through grant No. DMR-0427538. SCM gratefully acknowledges the support of the Texas Center for Superconductivity of the University of Houston ($T_c\text{SuH}$). The Advanced Photon Source is supported by the U.S. DOE, BES-DMS, under contract W-31-109-ENG-38.

* Currently at Carl Zeiss SMT AG, Lithography Optics Division, Rudolf-Eber-Straße 2, D-73447 Oberkochen, Germany

¹ I. M. Dubrovskii and M. A. Krivoglaz, Zh. Eksp. Teor. Fiz. Sov. Phys. JETP **77**, 1017 (1979).

² A. L. Korzhenevskii, K. Herrmanns and H.-O. Heuer, Europhys. Lett. **45**, 195 (1999).

³ S. R. Andrews, J. Phys. C **19**, 3721 (1986).

⁴ D. F. McMorrow, N. Hamaya, S. Shimomura, Y. Fujii, S. Kishimoto, H. Iwasaki, Solid State Commun. **76**, 443 (1990).

⁵ P. M. Gehring, K. Hirota, C. F. Majkrzak, G. Shirane, Phys. Rev. Lett. **71**, 1087 (1993).

⁶ T. R. Thurston, G. Helgesen, D. Gibbs, J. P. Hill,

- B. D. Gaulin, G. Shirane, Phys. Rev. Lett. **70**, 3151 (1993).
- ⁷ K. Hirota, G. Shirane, P. M. Gehring, C. F. Majkrzak, Phys. Rev. B **49**, 11967 (1994).
- ⁸ K. Hirota, J. P. Hill, S. M. Shapiro, G. Shirane, Y. Fujii, Phys. Rev. B **52**, 13195 (1995).
- ⁹ H.-B. Neumann, U. Rutt, J. R. Schneider, G. Shirane, Phys. Rev. B **52**, 3981 (1995).
- ¹⁰ R. A. Cowley, Physica Scripta **T66**, 24 (1996).
- ¹¹ P. M. Gehring, A. Vigilante, D. F. McMorrow, D. Gibbs, C. F. Majkrzak, G. Helgesen, R. A. Cowley, R. C. C. Ward, M. R. Wells, Physica B **221**, 398 (1996).
- ¹² U. Rütt, A. Diederichs, J. R. Schneider, G. Shirane, Europhysics Letters **39**, 395 (1997).
- ¹³ R. H. Wang, Y. M. Zhu, S. M. Shapiro, Phys. Rev. Lett. **80**, 2370 (1998).
- ¹⁴ J. Trenkler, P. C. Chow, P. Wochner, H. Abe, K. E. Bassler, R. Paniago, H. Reichert, D. Scarfe, T. H. Metzger, J. Peisl, J. Bai, S. C. Moss, Phys. Rev. Lett. **81**, 2276 (1998).
- ¹⁵ J. Trenkler, R. Barabash, H. Dosch and S. C. Moss, Phys. Rev. B **64** (2001) 214101.
- ¹⁶ T. Schober and W. Pesch, Zeit. Phys. Chem. - Wiesbaden **114**, 21 (1979).
- ¹⁷ J. Trenkler, H. Abe, P. Wochner, D. Haeffner, J. Bai, H. D. Carstanjen, S. C. Moss, Modelling Simul. Mater. Sci. Eng. **8**, 269 (2000).
- ¹⁸ J. Trenkler, S. C. Moss, H. Reichert, R. Paniago, U. Gebhardt, H. D. Carstanjen, T. H. Metzger, J. Peisl, in *Proceedings of the International Advanced Studies Institute Conference on Exploration of Subsurface Phenomena by Particle Scattering (ASI-002), Monterey, 1998*, edited by N. Q. Lam, C. A. Melendres and S. K. Sinha (IASI Press, North East, MD, 2000), p. 155.
- ¹⁹ L. H. Schwartz and J. B. Cohen, *Diffraction from materials* (Springer-Verlag, Berlin, 1987).
- ²⁰ B. Schönfeld, S. C. Moss and K. Kjær, Phys. Rev. B **36**, 5466 (1987).
- ²¹ D. Lawrie and S. Sarbach, in *Phase transitions and critical phenomena*, edited by C. Domb and J. L. Lebowitz (Academic Press, London, 1984), Vol. 9.
- ²² D. R. Nelson and M. E. Fisher, Phys. Rev. B **11**, 1030 (1975).
- ²³ W. B. Yelon, D. E. Cox, P. J. Kortman, W. B. Daniels, Phys. Rev. B **9**, 4843 (1974).
- ²⁴ M. A. Krivoglaz, *Diffuse scattering of X-rays and neutrons by fluctuations* (Springer-Verlag, Berlin, 1996).